J Mater Sci (2016) 51:5008–5018
DOI 10.1007/s10853-016-9805-y

Inherently flame-retardant flexible bio-based polyurethane sealant with phosphorus and nitrogen-containing polyurethane prepolymer

Haiyang Ding[1,2,3,4] · Chenglong Xia[1,2,3,4] · Jifu Wang[1,2,3,4] · Chunpeng Wang[1,2,3,4] · Fuxiang Chu[1,2,3,4,5]

Received: 2 December 2015 / Accepted: 1 February 2016 / Published online: 10 February 2016

Abstract A novel phosphorus and nitrogen-containing flame-retardant polyurethane prepolymer (FRPUP) was successfully synthesized and characterized by FTIR, ^{1}H NMR, and ^{31}P NMR. The flame-retardant polyurethane sealants (FRPUS) were prepared by curing FRPUP with castor oil. The flame-retardant properties of samples were investigated by the limiting oxygen index and cone calorimeter testing (CCT). The results showed that FRPUP can improve the flame retardancy of polyurethane sealants (PUS). The thermal decomposition behavior of the PUS was investigated by thermogravimetric analysis. Moreover, the thermal degradation mechanisms of FRPUS were investigated by thermogravimetric analysis/infrared spectrometry, FTIR, and X-ray photoelectron spectroscopy. The results indicated that the good flame retardancy of FRPUS can be attributed to the synergistic effect of phosphorus and nitrogen in FRPUP.

✉ Fuxiang Chu
chufuxiang@caf.ac.cn

Chunpeng Wang
wangcpg@163.com

[1] Institute of Chemical Industry of Forestry Products, CAF, Nanjing, China

[2] Key Laboratory of Biomass Energy and Material, Nanjing, Jiangsu, China

[3] National Engineering Laboratory for Biomass Chemical Utilization, Nanjing, China

[4] Key and Open Laboratory on Forest Chemical Engineering, SFA, Nanjing 210042, China

[5] Chinese Academy of Forestry, Beijing 100091, China

Introduction

Because of the good chemical resistance, mechanical strength, and affordable cost, polyurethane sealants (PUS) have attracted more and more attentions in recent years. It has been widely used as a sealing material in electronic components, construction, and automobile industry [1–3]. Among them, castor oil (CO)-based PUS (CO-PUS) play a dominant role due to its excellent electric insulating properties, strength, and less environmental pollution [4, 5]. However, high flammability of CO-PUS limits its applications. Thus, some research is required to improve the flame retardancy of CO-PUS for their comprehensive applications.

Over the past decades, additive-type flame retardants have been found to be an effective method to improve the flame retardancy of PUS [6]. However, the high concentration of the additive-type flame retardants in PUS has many drawbacks, such as poor compatibility, easy leaching, and a declining mechanical properties [7, 8]. Thus, more attentions have been paid to develop reactive-type flame retardants to replace additive-type flame retardants. In general, the reactive-type flame retardants with phosphorus, nitrogen, or silicon elements were introduced onto the molecule backbone of PUS to improve the flame retardancy of resins by chemical reaction [9–12].

In addition to phosphorus-based reactive-type flame retardants, phosphorus-nitrogen flame-retardant synergism system was reported in many literature and exhibited better flame-retardant efficiency than those only containing phosphorus, due to the synergistic effect between phosphorus and nitrogen. Chen et al. used 2-carboxyethyl(phenyl)phosphinic acid with melamine to synthesize phosphorus and nitrogen-containing flame-retardant additive for polyurethane foam [13]. Qian et al. synthesized phosphorus and

nitrogen-containing epoxy acrylate resin by the chemical reaction between phosphorus oxychloride ($POCl_3$), 2-hydroxyethyl acrylate (HEA), and piperazine. All the LOI values were found to be improved, which result from the synergistic effect of phosphorus and nitrogen [14–18]. However, phosphorus and nitrogen-containing compounds were rarely introduced onto the backbone of PUS and the synergistic effect between phosphorus and nitrogen in the condensed phase and gas phase during the combustion was rarely investigated.

In this study, a new flame-retardant polyurethane prepolymer (FRPUP) containing phosphorus and nitrogen was successfully synthesized and characterized. It was used as curing agent and reactive-type flame retardant for PUS (FRPUS). The flame retardancy of FRPUS was characterized by the LOI and CCT, and the thermal behavior of the FRPUS was studied by thermogravimetric analysis (TGA). In addition, TG-IR, RTIR, and XPS were used to analyze the flame-retardant mechanism and the degradation mechanism of FRPUS in both the gas phase and the condensed phase.

Experimental

Materials

Diethanolamine, formalin(37 % in water), Diethyl phosphite (DEPP), Dibutyltin dilaurate (DBTDL), Ethyl acetate (analytical grade) were purchased from Nanjing Chemical Reagents Co., Ltd. (Jiangsu, China). Castor oil (CO, hydroxyl value = 163; molecular weight = 933; average functionality = 2.7) was supplied by Nanjing Qianyue Chemicals Co., Ltd. (Jiangsu, China) and dried at 110 °C under vacuum for 2 h before use. Methylene diphenyl diisocyanate (MDI-50, NCO% = 32.6) was obtained from Yantai Wanhua Group Co., Ltd. (Shandong, China). BF-5(moisture scavenger) was supplied by Shanghai DEYUDE Trade Co., Ltd. (Shanghai, China). Defom 5500 (defoamer) was obtained from Guangzhou Shenggao Chemicals Co., Ltd. (Guangdong, China).

Synthesis of flame-retardant polyurethane prepolymer (FRPUP)

The FRPUP was prepared according to the previous report [16, 19]. Diethanolamine and formalin were added into a three-necked flask and stirred at 40 °C for 2 h. Then the mixture was heated to 80 °C to remove the generated water during the reaction under vacuum. Finally, DEPP was added into the above flask and stirred for another 2 h at 60 °C, the product (BHAPE) was obtained after being dried in a vacuum at 100 °C.

MDI-50 and a proper portion of DBTDL were dissolved in 30 mL of dried Ethyl acetate and charged into a four-necked round-bottomed flask and heated slowly to 70 °C under N_2 atmosphere. Then a solution of the BHAPE and 20 mL of dried ethyl acetate was slowly added into the above flask within 30 min, and the mixture was stirred for 2 h (The molar ratio of NCO and OH is 4.5:1, the NCO% of FRPUP is 20.3 %). The obtained product was referred as FRPUP. The synthesis route is illustrated in Scheme 1.

Preparation of flame-retardant PUS composites

The preparation of FRPUS composites was as follows: Firstly, a certain proportion of CO, DBTDL, BF-5, and Defom 5500 was added into a 500 mL plastic beaker at room temperature and stirred for 10 s. Then FRPUP (curing agent) was added into the mixtures in a certain ratio and stirred for another 10 s. Finally, the obtained viscous mixture was poured into a mold quickly and cured at 70 °C for 6 h. The compositions of FRPUS composites are summarized in Table 1. Other samples were prepared by the similar procedure.

Characterization

Fourier transform infrared (FTIR) spectroscopy

FTIR spectra of samples were recorded on a FTIR in a range of wave numbers from 4000 to 400 cm^{-1}, using attenuated total reflection Fourier transform infrared (ATR-FTIR) method on a Nicolet (USA) IS10 instrument.

Nuclear magnetic resonance spectroscopy (NMR) analysis

Nuclear magnetic resonance (NMR) measurement was performed on an AVANCE 400 Bruker spectrometer at room temperature. The solvent was $CDCl_3$.

Thermogravimetric analyses (TGA)

Thermogravimetric analyses was performed using a TGA Q500 (TA Instruments) instrument. About 4 mg of each sample was scanned from room temperature to 700 °C at a heating rate of 10 °C/min under nitrogen gas at a flow rate of 100 mL/min.

Limiting oxygen index (LOI)

LOI was carried out with a JF-3 oxygen index instrument (Jiangning Analysis Instrument Factory, Jiangsu, China), and the test was measured according to ASTM D2863. The samples used for the test were 120 × 10 × 10 mm^3.

Scheme 1 Synthesis route of FRPUP

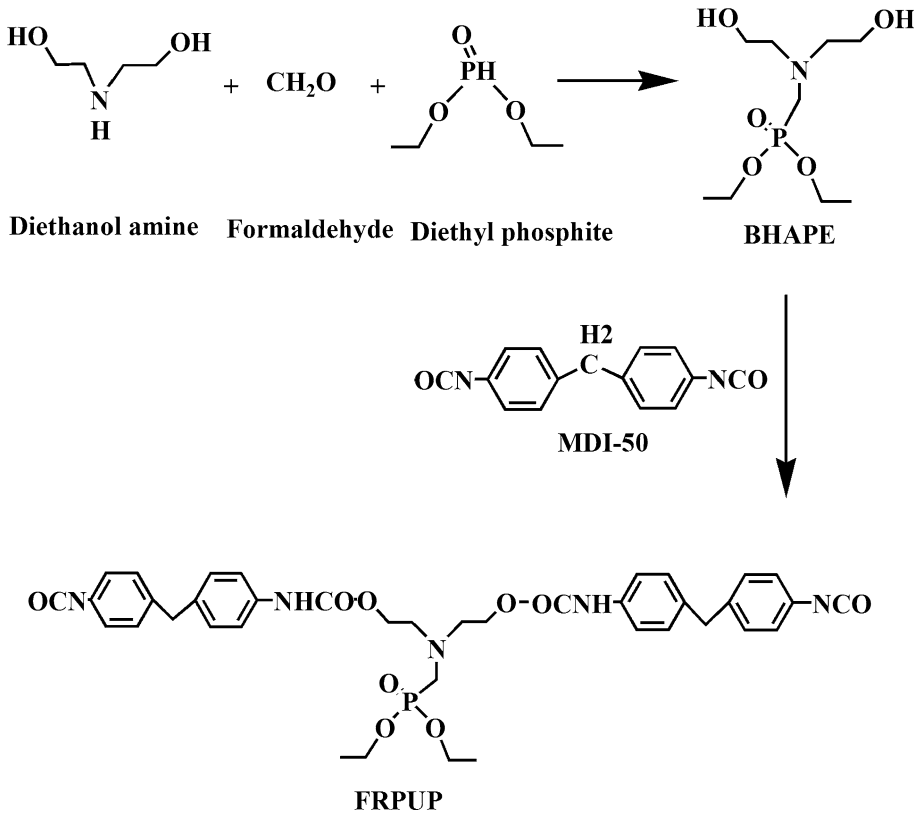

Table 1 Formulations of PUS

Samples	CO (g)	BF-5 (g)	Defom 5500 (g)	DBTDL (g)	MDI-50 (g)	FRPUP (g)
CO-PUS	10	0.01	0.01	0.005	3.9	0
FRPUS	10	0.01	0.01	0.005	0	6.3

Thermogravimetric analyses/infrared spectrometry (TG-IR)

TG-IR was performed using a TGA Q500 IR thermogravimetric analyzer, which was interfaced to the Nicolet (USA) IS10 FTIR spectrophotometer. About 4 mg of each sample was scanned from room temperature to 700 °C at a heating rate of 10 °C/min in nitrogen atmosphere.

Cone calorimeter testing (CCT)

The cone calorimeter tests of PUS were performed using an FTT2000 cone calorimeter instrument according to ISO 5660 standard. Each PUS specimens (100 × 100 × 10 mm^3) were irradiated at a heat flux of 35 kW/m^2.

X-ray photoelectron spectroscopy (XPS)

XPS was used to analyze the residual char, and it was carried out using a PHI 5000 VersaProbe (UlVAC-PHI Co., Ltd., Japan) with Al K*a* excitation radiation in ultrahigh vacuum conditions.

Result and discussion

Characterization

The FRPUP was prepared according to the previous report [16, 19]. The chemical structure of FRPUP was confirmed by FTIR, ^{1}H NMR, and ^{31}P NMR. As shown in Fig. 1, some specific absorption peaks are observed from FRPUP. The absorptions at 3300 and 2250 cm^{-1} is assigned to the N–H and -NCO, respectively. The absorption at 1728 cm^{-1} is attributed to the urethane bond. The absorption peaks at 1218 and 1018–960 cm^{-1} corresponding to the P=O stretching and the stretching vibrations of P-O-C, are clearly observed.

The ^{1}H NMR spectra of FRPUP are shown in Fig. 2, confirming the expected chemical structure. The ^{31}P NMR spectrum of the FRPUP is shown in Fig. 3. The peak at

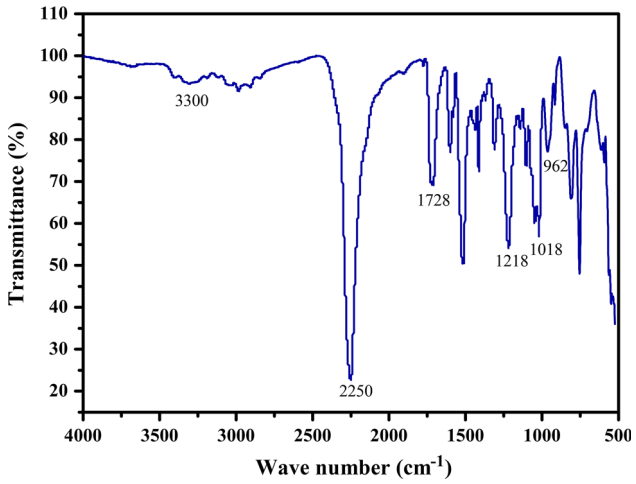

Fig. 1 FTIR spectra of FRPUP

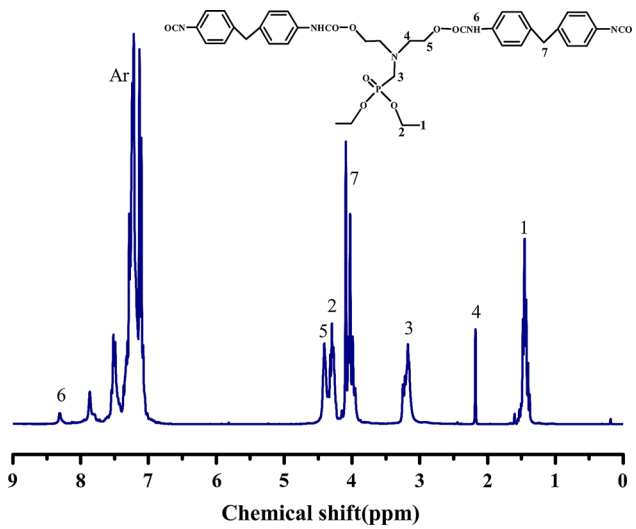

Fig. 2 ^{1}H NMR spectra of FRPUP

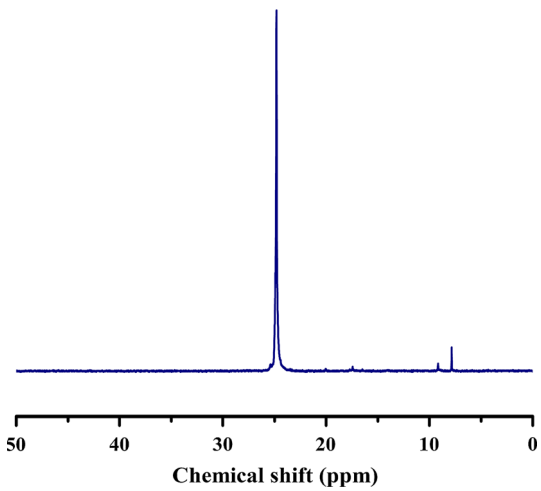

Fig. 3 ^{31}P NMR spectra of FRPUP

24.9 ppm belongs to the chemical shift of ^{31}P in the FRPUP structure [6]. These results suggest the successful synthesis of the FRPUP.

Thermal degradation behaviors

The thermal stability and thermal degradation of CO-PUS and FRPUS were investigated by TGA. The TGA curves mainly include the release of decomposition products and the formation of chars. Figure 4 shows their TGA thermograms in N_2, and the corresponding data are labeled in Table 2.

CO-PUS displays two main steps of degradation in N_2. The first stage occurred between 250 and 350 °C with a peak temperature of 328 °C, which may be due to the degradation of urethane bond [20, 21]. The second stage occurred between 350 and 500 °C and the maximum degradation rate happened at 408 °C, which is related to the degradation of PUS hydrocarbon chains [22]. Compared with CO-PUS, one step occurring between 250 and 350 °C in FRPUS is attributed to the decomposition of P-O-C bond at lower temperature. This phenomenon is probably due to the lower stability of P-O-C bond than C–C bond [23]. The temperatures of the maximum DTG peaks (T_{max}) for FRPUS are slightly higher than that of CO-PUS with the decreased maximum mass loss rate, indicating that FRPUS have higher thermal stability than CO-PUS [24].

Furthermore, Table 2 depicts the char residue of CO-PUS and FRPUS. It can be seen that the char residue of CO-PUS at 700 °C is only 1.5 %, while the char residue of FRPUS at 700 °C increases to 7.2 %. This phenomenon is probably due to the phosphorus and nitrogen elements in FRPUP acting as char-forming catalyst and synergistic agent, respectively. They can accelerate the formation of char during the decomposition process, indicating that

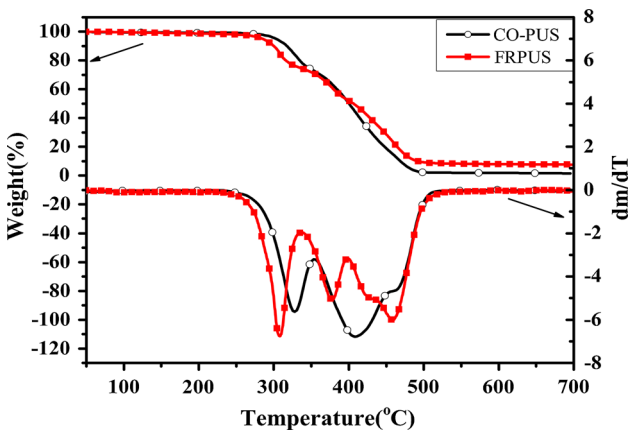

Fig. 4 TGA and DTG curves of the CO-PUS and FRPUS in N_2

Table 2 TGA date for CO-PUS and FRPUS in N_2

Samples	$T_{-5wt\%}$ (°C)	T_{max1} (°C)	R_{Tmax1} (%/min)	T_{max2} (°C)	R_{Tmax2} (%/min)	T_{max3} (°C)	R_{Tmax3} (%/min)	$C_{700\ °C}$ (%)
CO-PUS	303	–	–	328	5.6	408	6.8	1.5
FRPUS	268	308	5.63	378	5.0	459	6.0	7.2

$T_{5\ \%}$ 5 % is weight loss temperature, T_{max} is maximum weight loss temperature, R_{Tmax} is the weight loss rate at T_{max}, $C_{700\ °C}$ represents the char residue at 700 °C

Table 3 Cone calorimeter date for CO-PUS and FRPUS

Samples	PHRR (Kw/M^2)	THR (MJ/m^2)	Av-EHC (MJ/kg)	Av-MLR (g/s)	TSP (m^2)	LOI (%)
CO-PUS	1294	386	29.4	0.082	70.7	18.3
FRPUS	673	333	31.0	0.062	77.6	23.0

FRPUP could enhance the char yield and protect the underlying materials from further degradation [1, 17].

Burning behaviors

To evaluate the flame-retardant property of PUS, LOI was conducted, and the corresponding data are given in Table 3. From LOI data, CO-PUS has a LOI value of 18.3, while FRPUS exhibit a higher LOI value (23.1) [5, 25]. This indicates that incorporating phosphorus and nitrogen elements into the backbone of FRPUP effectively enhanced the flame retardancy of PUS [14].

In order to further evaluate the flammability behavior of PUS, cone calorimeter tests were performed for CO-PUS and FRPUS [10, 18]. Cone calorimeter is able to bring quantitative analysis to the flammability of materials by investigation parameters such as the peak heat release rate (PHRR), the heat release rate (HRR), the total heat release (THR), the rate of smoke release (RSR), the total smoke production (TSP), the average effective heat of combustion of volatiles (Av-EHC), and the average mass loss rate (Av-MLR).

The HRR, THR, RSR, and TSP curves of CO-PUS and FRPUS are shown in Figs. 5 and 6, and the corresponding data are presented in Table 3. From Fig. 5 and Table 3, it is observed that the CO-PUS burned rapidly and its PHRR and THR are 1294 kW/m^2 and 386 MJ/m^2, respectively. However, the HRR and THR curves of FRPUS increase rapidly at first and then decrease with much lower PHRR and THR values of 673 kW/m^2 and 333 MJ/m^2, which reduce by 48 and 14 % compared with that of CO-PUS. The reduction of the HRR and THR could probably be attributed to the char formation promoted by phosphorus element in FRPUR, which slows heat and mass transfer between the gas and condensed phases. It can be seen from Fig. 7a and b that the FRPUS have more char residue than that of CO-PUS, in which almost no char was generated. Figure 6 shows that the RSR curves have the similar trend to the HRR curves, and the TSP value of FRPUS increased to 77.6 from 70.7 m^2 for CO-PUS, indicating that FRPUS produced more smoke than did CO-PUS. This is probably that the much char layer protected the underlying material from further burning, which resulted in insufficient combustion and more smoke is produced [26].

Table 3 shows that the Av-EHC of FRPUS is higher than that of CO-PUS, which represented the greater amount of gases decomposed from FRPUS; the result is in accord with that of TSP. The Av-MLR of FRPUS is lower than that of CO-PUS, and they are 0.062 and 0.082 g/s, respectively. This phenomenon demonstrates that FRPUP mainly plays a role in the condensed phase.

Structural characterization of volatilized products

The gaseous thermal degradation products of CO-PUS and FRPUS were analyzed by TG-FTIR.

Figure 8 shows the 3D TG-FTIR spectra of gas phase in thermal degradation of CO-PUS (a) and FRPUS (b) at heating rate 10 °C/min in nitrogen atmosphere [13]. From Fig. 8a and b, it can be seen that peaks in the regions of 3600–4000, 2700–3100, 2100–2400, and 600–780 cm^{-1} are noted. Some of the gaseous decomposition products are unambiguously identified by characteristic FTIR signals, such as aromatic compounds (650–780 cm^{-1}), CO (2100–2200 cm^{-1}), CO_2 (2300–2400 cm^{-1}), and hydrocarbons (2850–3000 cm^{-1}) [20, 27].

FTIR spectra of pyrolysis products of CO-PUS and FRPUS at the maximum release rate are shown in Fig. 9. The main gas decomposition products of CO-PUS are compounds containing –OH (such as H_2O; 3600–3900 cm^{-1}), $-CH_3$ or $-CH_2$ (2929, 2856 cm^{-1}), CO_2 (2356 cm^{-1}), CO (2132 cm^{-1}), and aromatic rings (1450–1700, 750 cm^{-1}). The FRPUS release similar decomposition products to that of CO-PUS. Additionally, the new absorption bonds of FRPUS at 1221 and 1095 cm^{-1} appears, which are due to the structures of P=O and P–O–P, respectively. So, it can be concluded that the FRPUP in FRPUS decomposed to form polyphosphate and

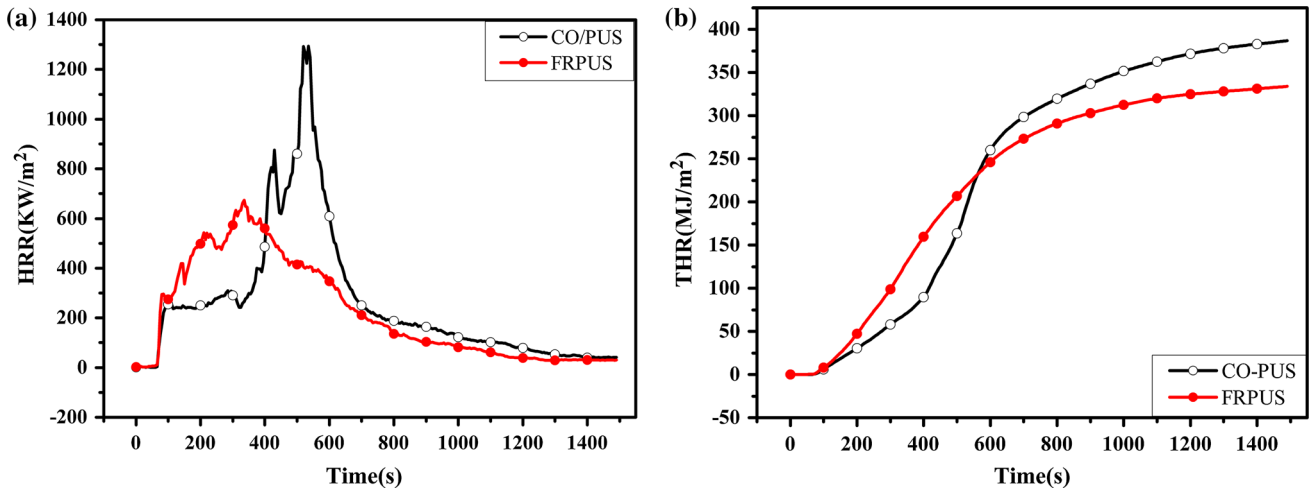

Fig. 5 HRR and THR curves of CO-PUS and FRPUS

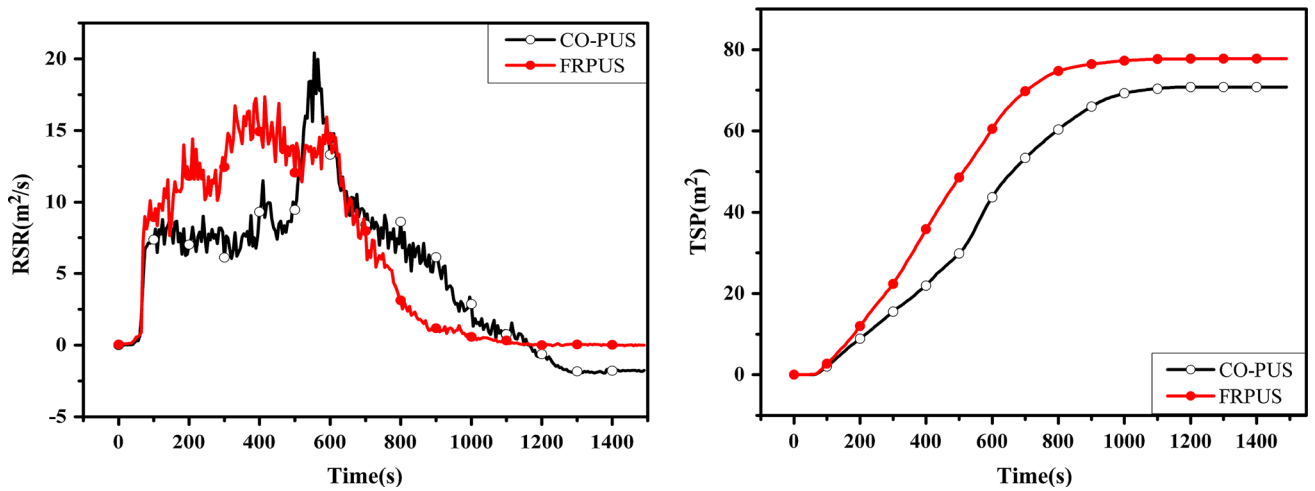

Fig. 6 RSR and TSP curves of CO-PUS and FRPUS

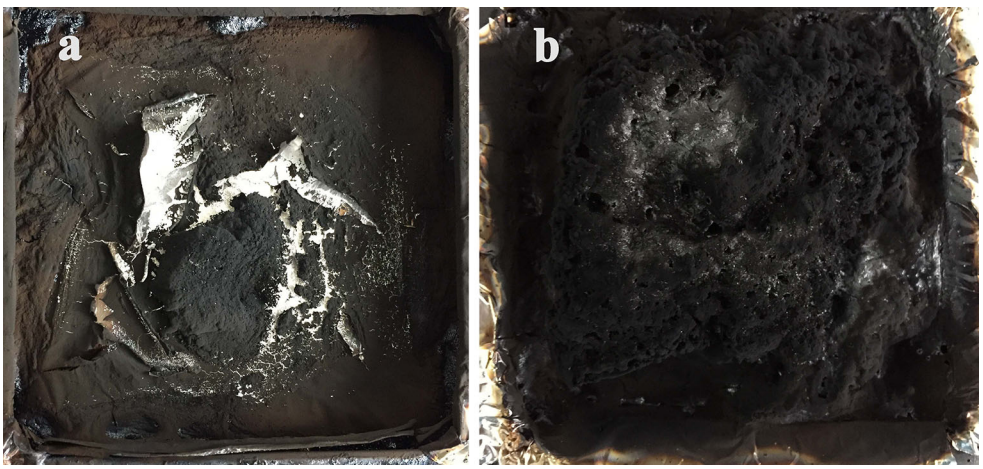

Fig. 7 Photographs of char residues of CO-PUS (**a**) and FRPUS (**b**)

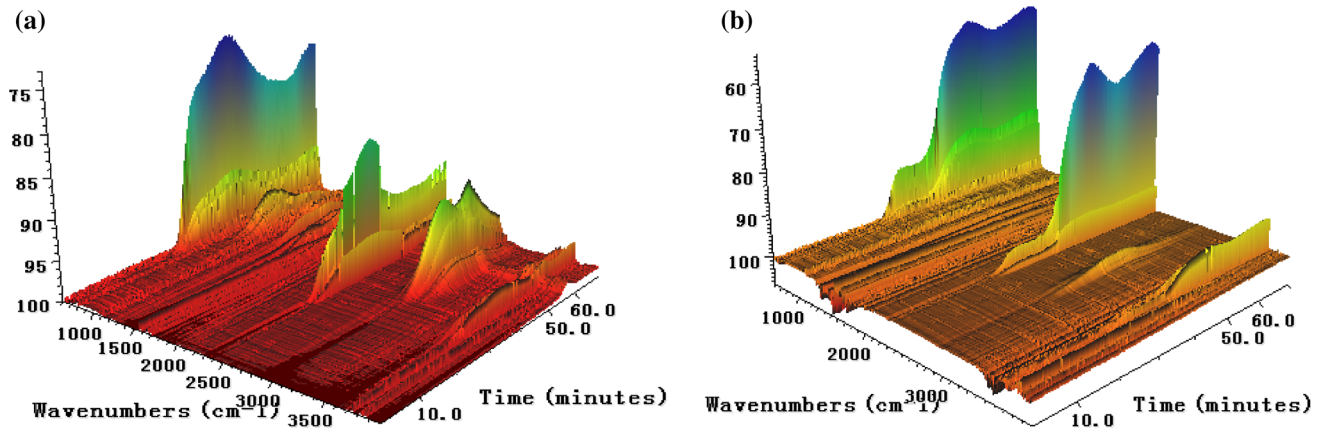

Fig. 8 The 3D TG-IR spectra of gas phase in the thermal decomposition of **a** CO-PUS and **b** FRPUS

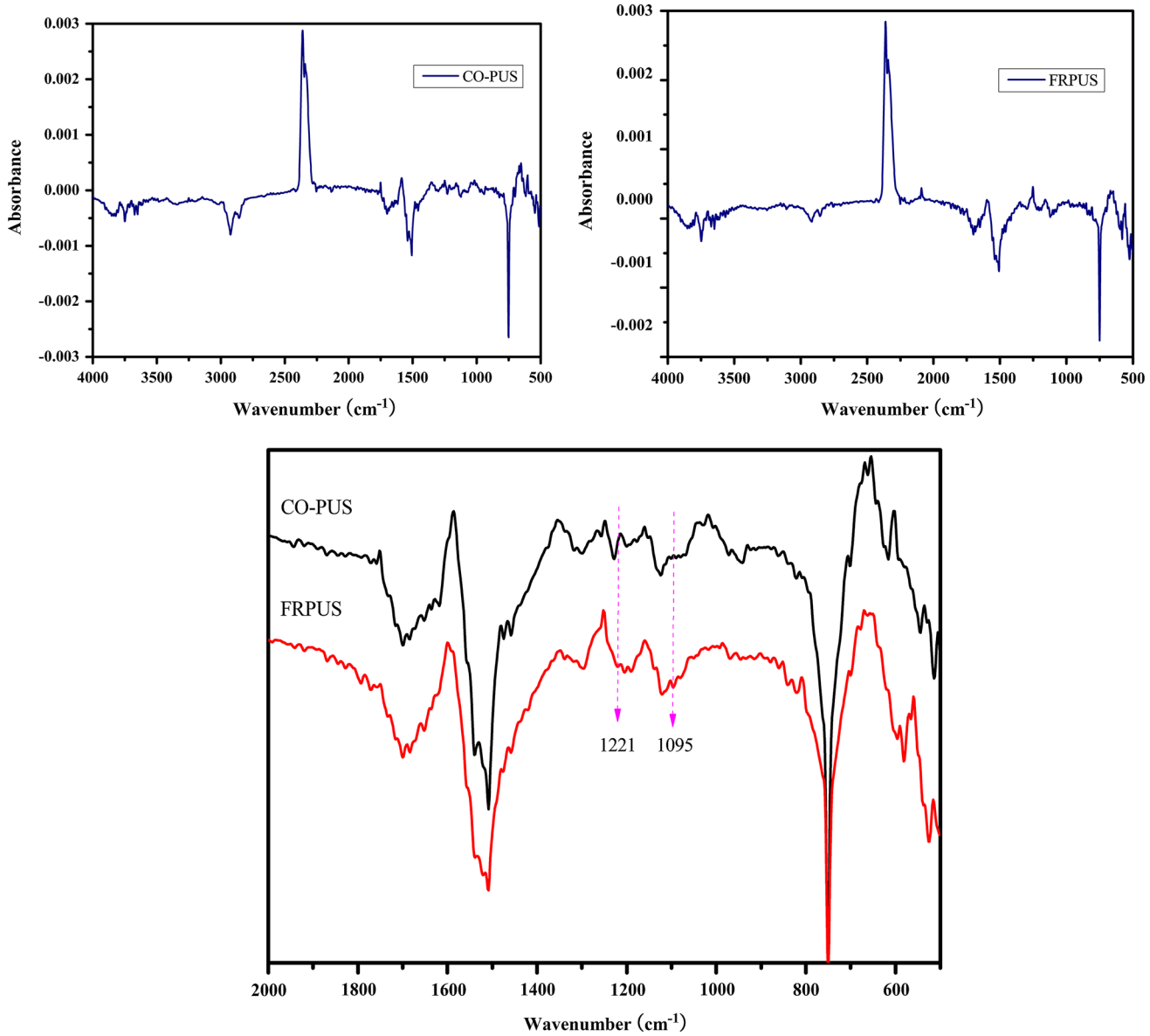

Fig. 9 The TG-IR spectra of gas phase in the thermal degradation of CO-PUS and FRPUS at the maximum decomposition rate

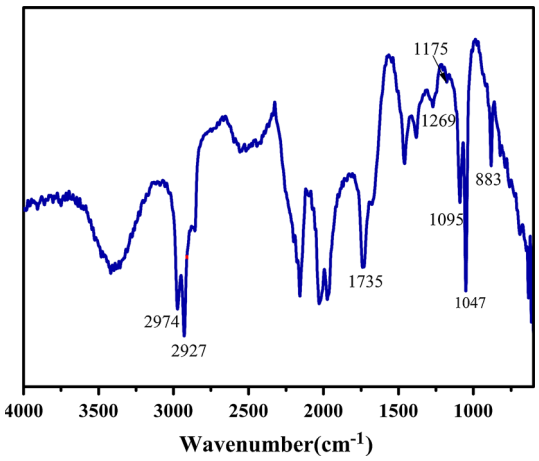

Fig. 10 FTIR spectrum of FRPUS char residue

phosphoric derivatives, which could promote the formation of a protective char layer [28, 29].

Analysis of the residual chars

To further investigate the combustion behavior of FRPUS and the flame-retardant mechanism, the structure of the char after CCT was examined by FTIR and XPS.

The FTIR spectrum of FRPUS char is shown in Fig. 10. It can be observed that-CH_3or -CH_2 groups (2974, 2927 cm^{-1}) C=O groups (1735 cm^{-1}), P=O groups (1269 cm^{-1}), P-O-C groups (1047 cm^{-1}), and P-O-P groups (1095, 883 cm^{-1}) existed in the char. These results show that the phosphate segments in FRPUP probably decomposed cross-linked phosphoric acid derivatives,

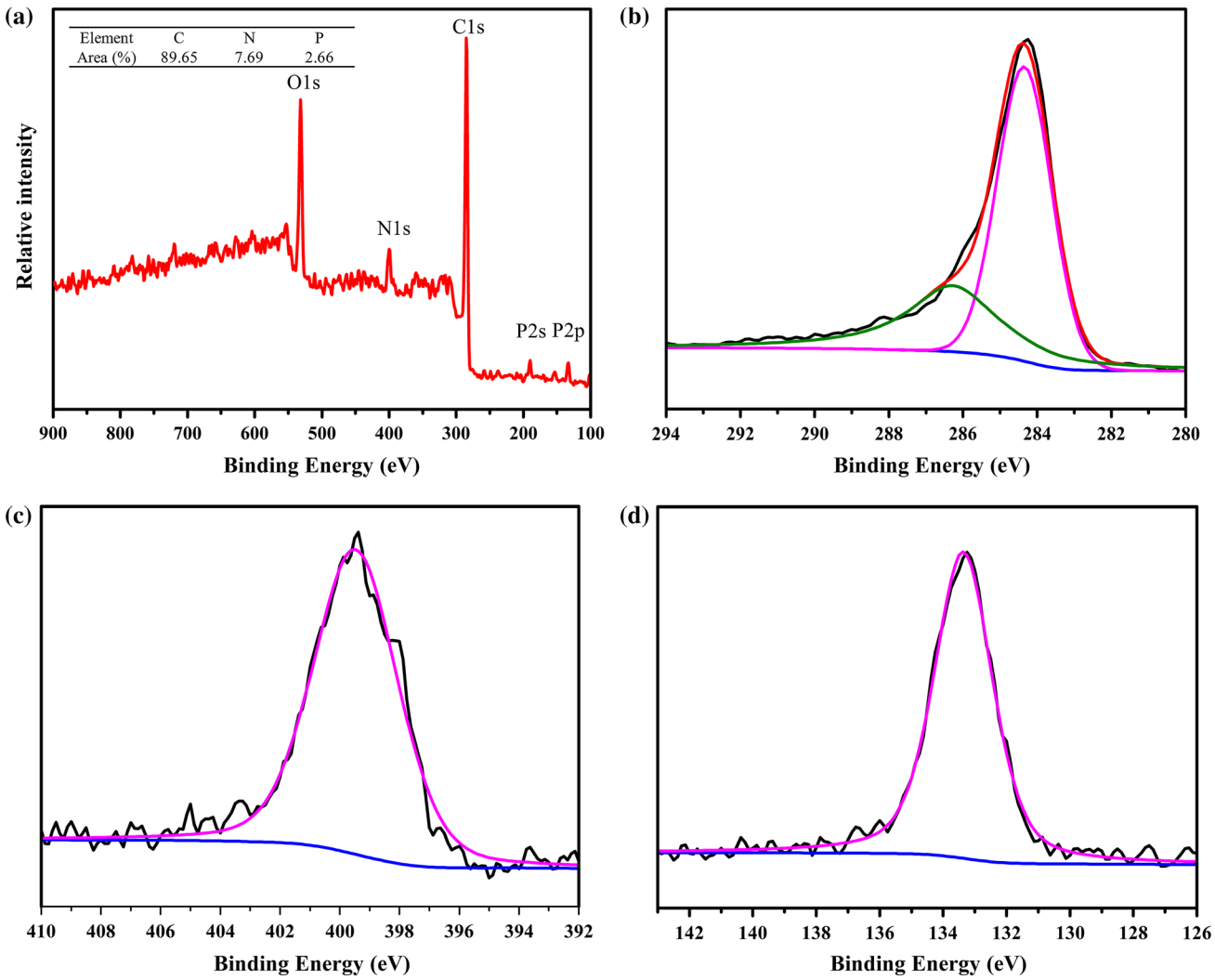

Fig. 11 **a** XPS spectrum and **b** C_{1s}, **c** N_{1s} and **d** P_{2p} XPS spectra of residual char of FRPUS

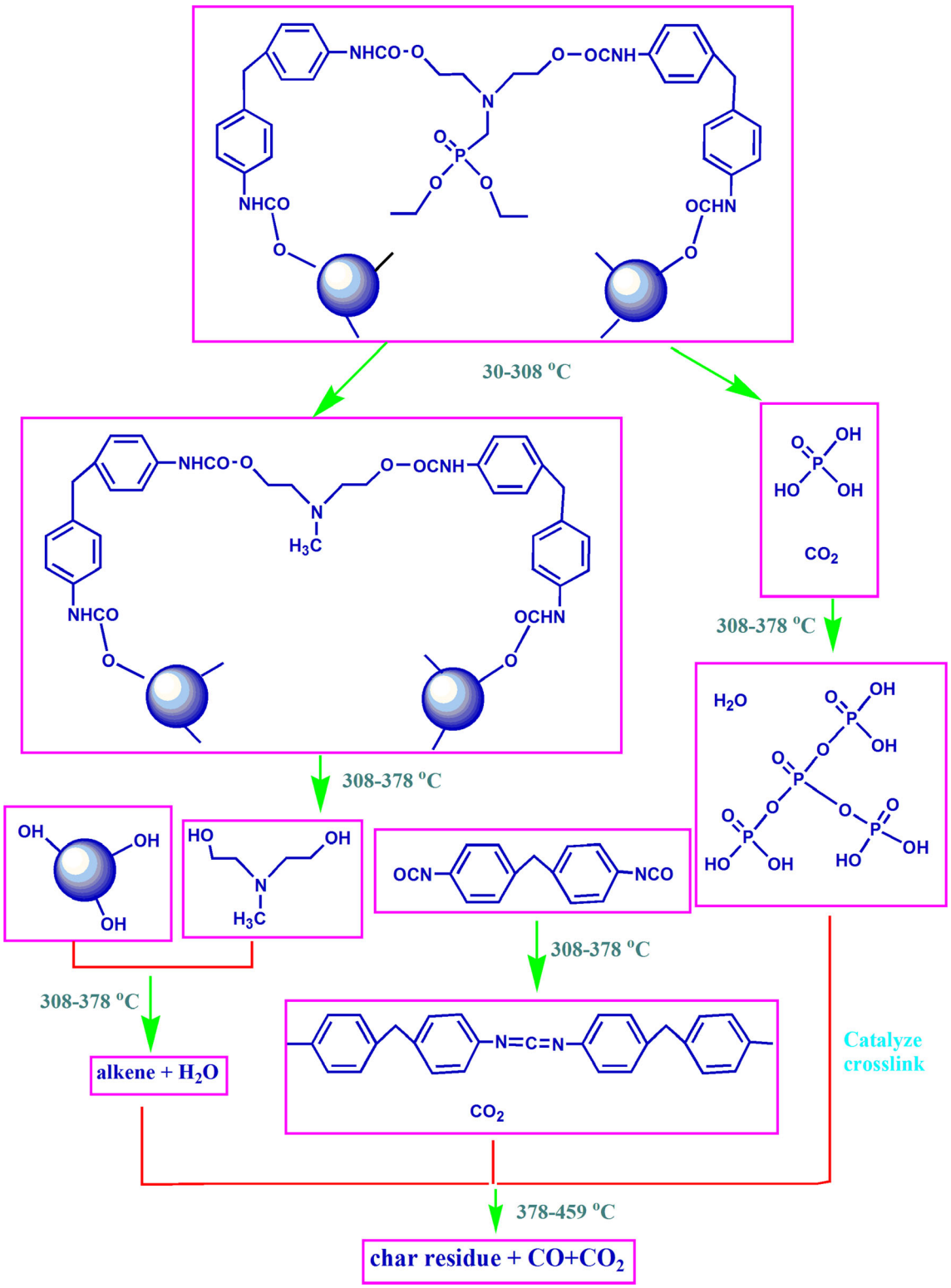

Scheme 2 Possible thermal degradation mechanism of FRPUS

which could promote the formation of char residues [7] (Fig. 10).

The XPS spectra of C_{1s}, N_{1s}, and P_{2p} of FRPUS are shown in Fig. 11. The residual char of FRPUS mainly contains carbon, nitrogen, oxygen, and phosphorus from FRPUP. The peak at 284.6 eV is attributed to C–C and C-H in aliphatic and aromatic species. The peak at 286.3 eV should be assigned to C-O in C-O-P. The peak at

Table 4 Mechanical and flame properties of CO-PUS and FRPUS

Samples	Hardness (Shore A)	Tensile strength (Mpa)	Elongation at break values (%)	NCO:OH (mol:mol)
CO-PUS	64	6.1	276.5	1.05:1
FRPUS	58	3.4	482.2	1.05:1

400 eV can be assigned to the N_{1s} of nitrogen compounds in the residual char. The peak at 133.4 eV from P_{2p} spectrum is attributed to the pyrophosphate and/or polyphosphate, which could promote the carbonization of FRPUS [5, 9, 26, 30, 31].

According to the results of TG, TG-IR, FTIR, and XPS, the possible thermal degradation mechanism of FRPUS is shown in Scheme 2. First, from room temperature to 308 °C, the P-O-C and P–C bonds in FRPUP were broken and formed phosphoric acid and some H_2O, CO_2. Second, at 308–378 °C, the urethane groups formed between CO and FRPUP are decomposed into isocyanate and hydroxyl compounds. With the temperature increase, isocyanate and hydroxyl compounds can further form carbodiimides and hydrocarbon compounds (alkane, alkene) with the evolution of H_2O and CO_2. At the same time, the phosphoric acid compounds can form polyphosphoric acid, which could accelerate the formation of char as catalyst. Finally, at 378–459 °C, a stable char layer containing phosphorus species and polyaromatic structures is obtained in the presence of polyphosphoric acid, and the volatilized CO and CO_2 are released [7, 11, 15, 16, 26].

Mechanical properties

The mechanical properties are characterized by universal testing machine according to the GB/T2411-2008 and GB/T 13022-91 standards. The mechanical properties of the PUS including hardness, tensile strength, and elongation at break are listed in Table 4 [26]. FRPUS exhibit lower hardness and tensile strength than CO-PUS. However, FRPUS show a higher value for elongation at break than CO-PUS. This phenomenon can be attributed to the fact that FRPUP has some longer molecular chain than MDI-50, which resulted in the lower cross-linking density than CO-PUS [32, 33].

Conclusions

In this work, a novel phosphorus- and nitrogen-containing polyurethane prepolymer (FRPUP) was successfully synthesized and applied in PUS. The chemical structure of FRPUP was confirmed by FTIR, ^{1}H NMR, and ^{31}P NMR. The resulting FRPUS demonstrated significant enhancements in thermal properties, flame retardancy, and combustion properties. The thermal degradation of FRPUS was studied by TGA and TG-IR. It was found that FRPUP can greatly enhance the char residues of PUS, which was caused by the synergistic effect of P and N elements in FRPUP. The study of flammability of FRPUS revealed that FRPUP could increase the LOI value and decrease the PHRR and THR. The residues were analyzed by FTIR and XPS, and the results indicated that phosphorus elements in FRPUP could catalyze the cross-linking reaction and form a stable char at high temperature. Furthermore, FRPUP can enhance the toughness of PUS.

Acknowledgements This work was supported by the forest research and special public service foundation (Grand No. 201404604).

References

1. Gao L, Zheng G, Zhou Y, Hu L, Feng G, Zhang M (2014) Synergistic effect of expandable graphite, diethyl ethylphosphonate and organically-modified layered double hydroxide on flame retardancy and fire behavior of polyisocyanurate-polyurethane foam nanocomposite. Polym Degrad Stab 101:92–101. doi:10.1016/j.polymdegradstab.2013.12.025
2. Liu Y, Zhao J, Deng C-L, Chen L, Wang D-Y, Wang Y-Z (2011) Flame-retardant effect of sepiolite on an intumescent flame-retardant polypropylene system. Ind Eng Chem Res 50:2047–2054. doi:10.1021/ie101737n
3. Li Y, Li B, Dai J, Jia H, Gao S (2008) Synergistic effects of lanthanum oxide on a novel intumescent flame retardant polypropylene system. Polym Degrad Stab 93:9–16. doi:10.1016/j.polymdegradstab.2007.11.002
4. Seeni Meera KM, Murali Sankar R, Jaisankar SN, Mandal AB (2013) Physicochemical studies on polyurethane/siloxane cross-linked films for hydrophobic surfaces by the sol-gel process. J Phys Chem B 117:2682–2694. doi:10.1021/jp3097346
5. Ke C-H, Li J, Fang K-Y et al (2010) Synergistic effect between a novel hyperbranched charring agent and ammonium polyphosphate on the flame retardant and anti-dripping properties of polylactide. Polym Degrad Stab 95:763–770. doi:10.1016/j.polymdegradstab.2010.02.011
6. Liao F, Zhou L, Ju Y, Yang Y, Wang X (2014) Synthesis of a novel phosphorus-nitrogen-silicon polymeric flame retardant and its application in poly(lactic acid). Ind Eng Chem Res 53:10015. doi:10.1021/ie5008745
7. Chen M-J, Chen C-R, Tan Y et al (2014) Inherently flame-retardant flexible polyurethane foam with low content of phosphorus-containing cross-linking agent. Ind Eng Chem Res 53:1160. doi:10.1021/ie4036753
8. Lu S-Y, Hamerton I (2002) Recent developments in the chemistry of halogen-free flame retardant polymers. Prog Polym Sci 27:1661. doi:10.1016/S0079-6700(2)00018-7
9. Bai Z, Song L, Hu Y, Yuen RK (2013) Preparation, flame retardancy, and thermal degradation of unsaturated polyester

resin modified with a novel phosphorus containing acrylate. Ind Eng Chem Res 52:12855. doi:10.1021/ie401662x
10. Tang Q, Yang R, He J (2014) Investigations of thermoplastic poly(imide-urethanes) flame-retarded by hydroxyl-terminated poly(dimethylsiloxane). Ind Eng Chem Res 53:9714. doi:10.1021/ie500473t
11. Cao K, S-l W, S-l Qiu Y, Li ZY (2012) Synthesis of N-alkoxy hindered amine containing silane as a multifunctional flame retardant synergist and its application in intumescent flame retardant polypropylene. Ind Eng Chem Res 52:309. doi:10.1021/ie3017048
12. Wang X, Zhan J, Xing W et al (2013) Flame retardancy and thermal properties of novel UV-curable epoxy acrylate coatings modified by a silicon-bearing hyperbranched polyphosphonate acrylate. Ind Eng Chem Res 52:5548. doi:10.1021/ie3033813
13. Chen M-J, Shao Z-B, Wang X-L, Chen L, Wang Y-Z (2012) Halogen-free flame-retardant flexible polyurethane foam with a novel nitrogen-phosphorus flame retardant. Ind Eng Chem Res 51:9769. doi:10.1021/ie301004d
14. Bai Y, Wang X, Wu D (2012) Novel cyclolinear cyclotriphosphazene-linked epoxy resin for halogen-free fire resistance: synthesis, characterization, and flammability characteristics. Ind Eng Chem Res 51:15064. doi:10.1021/ie300962a
15. Chen L, Song L, Lv P et al (2011) A new intumescent flame retardant containing phosphorus and nitrogen: preparation, thermal properties and application to UV curable coating. Prog Org Coat 70:59. doi:10.1016/j.porgcoat.2010.10.002
16. Jiang S, Shi Y, Qian X et al (2013) Synthesis of a novel phosphorus- and nitrogen-containing acrylate and its performance as an intumescent flame retardant for epoxy acrylate. Ind Eng Chem Res 52:17442. doi:10.1021/ie4028439
17. Qian X, Song L, Jiang S et al (2013) Novel flame retardants containing 9,10-dihydro-9-oxa-10-phosphaphenanthrene-10-oxide and unsaturated bonds: synthesis, characterization, and application in the flame retardancy of epoxy acrylates. Ind Eng Chem Res 52:7307. doi:10.1021/ie4028439
18. Qian X, Song L, Hu Y et al (2011) Combustion and thermal degradation mechanism of novel intumescent flame retardant for epoxy acrylate containing phosphorus and nitrogen. Ind Eng Chem Res 50:1881. doi:10.1021/ie400872q
19. Ding H, Wang J, Liu J et al (2015) Preparation and properties of a novel flame retardant polyurethane quasi-prepolymer for toughening phenolic foam. J Appl Polym Sci. doi:10.1002/app.42424
20. Bai Z, Song L, Hu Y, Gong X, Yuen RK (2014) Investigation on flame retardancy, combustion and pyrolysis behavior of flame retarded unsaturated polyester resin with a star-shaped phosphorus-containing compound. J Anal Appl Pyrol 105:317. doi:10.1016/J.JAPP.2013.11.019
21. Zhang M, Zhang J, Chen S, Zhou Y (2014) Synthesis and fire properties of rigid polyurethane foams made from a polyol derived from melamine and cardanol. Polym Degrad Stab 110:27. doi:10.1016/j.polymdegradstab.2014.08.009
22. Heinen M, Gerbase AE, Petzhold CL (2014) Vegetable oil-based rigid polyurethanes and phosphorylated flame-retardants derived from epoxydized soybean oil. Polym Degrad Stab 108:76. doi:10.1016/j.polymdegradstab.2014.05.024
23. Velencoso MM, Ramos MJ, Klein R, De Lucas A, Rodriguez JF (2014) Thermal degradation and flame behavior of novel polyurethanes based on phosphate polyols. Polym Degrad Stab 101:40. doi:10.1016/j.polymdegradstab.2014.01.012
24. Wang H, Wang Q, Huang Z, Shi W (2007) Synthesis and thermal degradation behaviors of hyperbranched polyphosphate. Polym Degrad Stab 92:1788. doi:10.1016/j.polymdegradstab.2007.07.008
25. Allauddin S, Narayan R, Raju K (2013) Synthesis and properties of alkoxysilane castor oil and their polyurethane/urea-silica hybrid coating films. ACS Sustain Chem Eng 1:910. doi:10.1021/sc3001756
26. Shao Z-B, Deng C, Tan Y, Chen M-J, Chen L, Wang Y-Z (2014) An efficient mono-component polymeric intumescent flame retardant for polypropylene: preparation and application. ACS Appl Mater Interfaces 6:7363. doi:10.1021/am500789q
27. Guo Y, Bao C, Song L, Yuan B, Hu Y (2011) In situ polymerization of graphene, graphite oxide, and functionalized graphite oxide into epoxy resin and comparison study of on-the-flame behavior. Ind Eng Chem Res 50:7772. doi:10.1021/ie200152x
28. Chen X, Jiao C (2008) Synergistic effects of hydroxy silicone oil on intumescent flame retardant polypropylene system. Polym Degrad Stab 93:2222. doi:10.1016/j.firesaf.2009.06.008
29. Li X-H, Meng Y-Z, Zhu Q, Tjong S (2003) Thermal decomposition characteristics of poly(propylene carbonate) using TG/IR and Py-GC/MS techniques. Polym Degrad Stab 81:157. doi:10.1016/S0141-3910(03)00085-5
30. Zhao W, Liu J, Peng H, Liao J, Wang X (2015) Synthesis of a novel PEPA-substituted polyphosphoramide with high char residues and its performance as an intumescent flame retardant for epoxy resins. Polym Degrad Stab 118:120. doi:10.1016/j.polymdegradstab.2015.04.023
31. Ohtsu N, Hiromoto S, Yamane M, Satoh K, Tomozawa M (2013) Chemical and crystallographic characterizations of hydroxyapatite- and octacalcium phosphate-coatings on magnesium synthesized by chemical solution deposition using XPS and XRD. Surf Coat Technol 218:114. doi:10.1016/j.surfcoat.2012.12.037
32. Miao S, Sun L, Wang P, Liu R, Su Z, Zhang S (2012) Soybean oil-based polyurethanes networks as candidate biomaterials: synthesis and biocompatibility. Eur J Lipid Sci Technol 114:1165. doi:10.1002/ejlt.201200050
33. Zhang C, Xia Y, Chen R, Huh S, Johnston PA, Kessler MR (2013) Soy-castor oil based polyols prepared using a solvent-free and catalyst-free method and polyurethanes therefrom. Green Chem 15:1477. doi:10.1039/C3GC40531A